Available online at www.sciencedirect.com
ScienceDirect
Journal of the European Ceramic Society 27 (2007) 2635–2640
www.elsevier.com/locate/jeurceramsoc

Thermal conductivity of alumina inclusion/glass matrix composite materials: local and macroscopic scales

N. Tessier-Doyen [a,*], X. Grenier [a], M. Huger [a], D.S. Smith [a], D. Fournier [b], J.P. Roger [b]

[a] *Groupe d'Etude des Matériaux Hétérogènes (GEMH, EA 3178), Ecole Nationale Supérieure de Céramique Industrielle, 47 à 73, Avenue Albert Thomas, 87065 Limoges Cedex, France*

[b] *Laboratoire d'Optique Physique, Ecole Supérieure de Physique et de Chimie Industrielles, 10, rue Vauquelin, 75005 Paris, UPR A0005 du CNRS, Université Pierre et Marie Curie, France*

Received 19 July 2006; received in revised form 19 September 2006; accepted 24 September 2006
Available online 20 November 2006

Abstract

The thermal conductivity of a two-phase material, based on a glass matrix containing mm sized spherical alumina inclusions, has been studied as a function of the alumina phase volume fraction. The glass matrix and the alumina phase were chosen with almost identical coefficients of thermal expansion to ensure good thermal contact at the interface between the two phases. The thermal conductivity of the alumina phase was determined by local measurements on the inclusions using the mirage technique. For the glass phase and the two-phase samples, the thermal conductivity values were evaluated with the laser flash technique and compared to predictions by analytical models. The Maxwell–Eucken model gives a close agreement to these experimental values for alumina volume fractions up to 55%. In fact, we show that for large mm sized alumina inclusions, Hasselman's correction for the interface thermal resistance is not necessary.

Keywords: Composites; Thermal conductivity; Glass; Two-phase materials

1. Introduction

Refractory parts are used to contain high temperature processes such as steel or glass manufacture and separate the molten liquid from the environment. Thermal insulation therefore constitutes an important function for some of the refractory materials in the system and is principally controlled by the thermal conductivity. Other parts of the refractory system can be subjected to severe temperature changes. Resistance to thermal shock is then a critical aspect for part lifetime and this is also related, though in a different way, to the thermal properties of a material. From the point of view of system performance and lifetime, numerical simulation of thermal and mechanical stresses occurring in operating conditions is increasingly used to optimise the design and material choice. However the approach requires, as data input, the macroscopic thermal and mechanical characteristics of the materials making up the system. We now focus on the value of effective thermal conductivity attributed to a refractory material with a complex microstructure consisting of a mixture of solid phases in granular form, the associated interfaces, pores and eventually cracks. All these features can influence the heat transfer though the heterogeneous solid and hence the effective thermal conductivity parameter value attributed to a material for simulation. Such a value can be obtained by experiment or by theoretical calculation if there is sufficient knowledge of the material constituents, microstructure, and thermal response at the local scale to allow the choice of a suitable model.

At the present time and state of available techniques, commonly used industrial materials such as an alumina-carbon or alumina-chrome refractories[1] provide too much complexity for non ambiguous conclusions to be drawn. Consequently, we have chosen to work with a model material constituted of two solid phases with a simplified microstructure. The ultimate aim is to incorporate the role of differences of thermal expansion coefficient on the thermal and mechanical characteristics of a heterogeneous material and hence on its thermal shock resistance.

* Corresponding author. Tel.: +33 5 5545 2222; fax: +33 5 5579 0998.
E-mail address: n_tessier-doyen@ensci.fr (N. Tessier-Doyen).

0955-2219/$ – see front matter © 2006 Elsevier Ltd. All rights reserved.
doi:10.1016/j.jeurceramsoc.2006.09.017

However in the present work, in order to fix the baseline for these further studies, the two phases have been chosen so that their coefficient of thermal expansion match as closely as possible. The chosen composite material is composed of alumina inclusions with a narrow size distribution dispersed in a glass matrix. Thermal conductivity evaluation has been performed both at local and macroscopic scales. The macroscopic experimental values are compared to those obtained with the Maxwell–Eucken model including Hasselman's correction for interface resistance and Landauer's effective medium expression. The importance of local microstructural detail on thermal response is revealed.

2. Experimental

2.1. Sample preparation

Glass/alumina samples were prepared using a borosilicate glass as the matrix. Glass powder was mixed with alumina beads and selected organic additives in a procedure which has been described previously.[2] The two constituents exhibit quite similar coefficients of thermal expansion (respectively 7.4×10^{-6} and $7.6 \times 10^{-6}\,K^{-1}$ in the temperature range 20–400 °C) to ensure good contact at the interfaces between the glass and alumina inclusions. As shown in Fig. 1a, the typical diameters of alumina inclusions range from 0.9 to 1.5 mm. Bars (50 mm × 10 mm × 10 mm) were prepared from the mixture by cold uni-axial pressing at 80 MPa. After debinding, the samples were hot-pressed (750 °C, 15 mn) to reduce the residual matrix porosity to less than 1%. Six imposed volume fractions of alumina inclusions (10, 20, 30, 40, 48 and 55%) were investigated (Table 2). Finally, three discs of 8 mm in diameter and 3 mm in thickness were cut from the bar (Fig. 1b). As the cutting of samples can lead to slight variations in the proportions of each phase in these smaller samples compared to the initial bars, the real volume fractions were recalculated from new measurements of the bulk density, assuming zero porosity (Table 2). These values, with an accuracy better than 1%, were comparable to those of the surface fractions determined by image analysis[2] and discussed in an other paper focused on elastic properties.

2.2. Thermal diffusivity–conductivity measurements

2.2.1. Laser flash technique

Thermal diffusivity measurements using the laser flash technique[3] were performed to evaluate the thermal conductivity of the matrix and the two-phase materials. For a given sample, the thermal conductivity is calculated from the value of its measured thermal diffusivity (a), its density (ρ) and its specific heat (c):

$$\lambda = \rho c a \tag{1}$$

The specific heat at room temperature of each two-phase sample was calculated with the rule of mixtures using literature values for the components[4].

2.2.2. Photo-thermal experiment: mirage set-up

Since the shape and the diameter of the alumina beads were not suitable for characterisation with the laser flash technique, diffusivity measurements were performed using a photo-thermal technique. Photo-thermal methods have the particularity of being able to determine the thermal diffusivity at different scales, from the micron to the millimetre. They are based on measuring local variations of temperature, which have been induced at the surface of the sample by the absorption of a modulated light flux. In the case of a point source, the solution of the heat diffusion equation for a semi-infinite homogeneous medium with a planar modulated heat source at $r = 0$ is given by

$$T(r,t) = \frac{T_0}{r}\, e^{-r/\mu}\, e^{j[2\pi f t - (r/\mu)]} \tag{2}$$

where $T(r,t)$ is the time dependent temperature at a distance r from the source, T_0 is proportional to the amplitude supplied by the heat source with modulation frequency f and the thermal diffusion length $\mu = \sqrt{a/\pi f}$ which characterizes the heat propagation in the medium.

If significant fluctuations in the sample microstructure are at a scale less than the micron, the photo-reflectance microscope is the most convenient technique. If not, as is the case for the sample under study, the only usable technique is mirage detection. In this technique, the surface temperature is deduced from

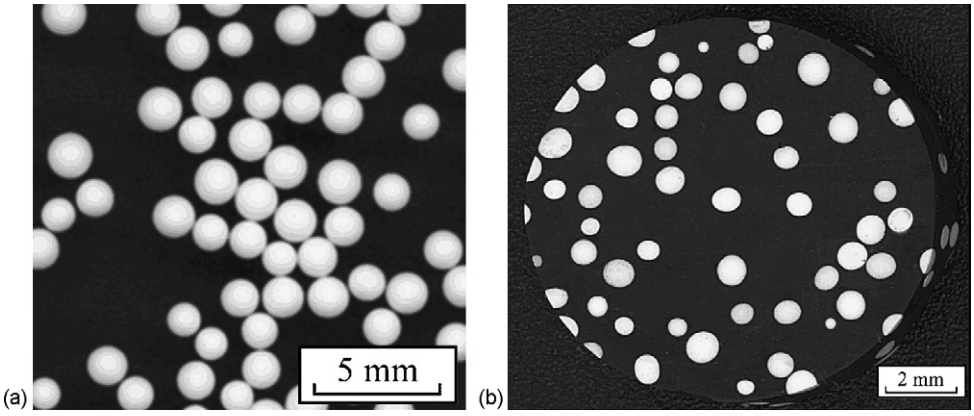

Fig. 1. (a) Scanned alumina beads; (b) a two-phase disc sample containing 20 vol.% of inclusions.

the deflection angle of a laser beam propagating parallel to the surface of the sample[5]. Small volumes of material, typically in the 0.1–1 mm dimension range for the diameter, can be probed and this is well suited to the characterization of alumina beads. The measurement of samples with low thermal conductivity is not so easy with the mirage set-up due to the large expansions of the periodically heated volume of air compared to the solid volume within the sample. The geometrical parameters of the measurement (beam diameters, sample surface—probe beam distance, etc.) have to be well known in order to obtain a precise value of the thermal diffusivity. The expected accuracy is around 15%.

3. Background analysis

3.1. Effect of grain boundaries on the equivalent thermal conductivity of alumina

The microstructure of a ceramic material can be approximated by a three-dimensional lattice of cubic cells. Based on symmetry with respect to a heat flow direction, the thermal resistance of a dense polycrystalline ceramic can be written:

$$R_{\text{poly}} = R_{\text{crystal}} + NR_{\text{int}} \tag{3}$$

where R_{crystal} is the thermal resistance of the single crystal, R_{int} that of the grain boundary and N the number of grain boundaries crossed by the heat flow. The following expression for the thermal conductivity of dense polycrystalline ceramic was experimentally validated for alumina:[6]

$$\lambda_{\text{poly}}^{-1} = \frac{1}{\lambda_{\text{crystal}}} + nR_{\text{int}}^{*} \tag{4}$$

where λ_{crystal} is the single crystal thermal conductivity, n the number of grain boundaries per unit length of heat flow path ($n = 1/\phi_{\text{grain}}$ with ϕ_{grain} the mean size of grains) and R_{int}^{*} the thermal resistance for a grain boundary of unit area. In this approach, it is assumed that scattering defects such as impurities, vacancies and dislocations are described by the single crystal term of Eq. (4).

3.2. Predicted effective thermal conductivity of a two-phase material

The upper and lower bounds for the effective thermal conductivity of a two-phase mixture can be calculated using parallel and series equivalent circuits, but these do not correspond to the real microstructure. The Maxwell–Eucken expression[7,8] can be used to describe the thermal conductivity of an arrangement of isolated spherical inclusions dispersed in a continuous homogeneous matrix and is given by

$$\lambda_{\text{eff}} = \lambda_{\text{m}} \left[\frac{\lambda_{\text{i}} + 2\lambda_{\text{m}} + 2v_{\text{i}}(\lambda_{\text{i}} - \lambda_{\text{m}})}{\lambda_{\text{i}} + 2\lambda_{\text{m}} - v_{\text{i}}(\lambda_{\text{i}} - \lambda_{\text{m}})} \right] \tag{5}$$

where v represents the volume fraction and the subscripts m and i refer, respectively to the matrix and to the inclusions. Interactions between the thermal fields around each inclusion are assumed to be negligible. This means that each particle should be located rather far from its nearest neighbours and the application of the expression should be restricted to small volume fractions of inclusions (<15 vol.%).

The effect of the thermal boundary resistance between the matrix and inclusions can be taken into account using the equation developed by Hasselman[9]. This involves a correction to Maxwell's theory and the predicted effective thermal conductivity for spherical inclusions in an otherwise homogeneous matrix is written in the following form:

$$\lambda_{\text{eff}} = \lambda_{\text{m}} \frac{2\left((\lambda_{\text{i}}/\lambda_{\text{m}}) - (\lambda_{\text{i}}/c)(1/h) - 1\right)v_{\text{i}} + (\lambda_{\text{i}}/\lambda_{\text{m}}) + (2\lambda_{\text{i}}/c)(1/h) + 2}{\left(1 - (\lambda_{\text{i}}/\lambda_{\text{m}}) + (\lambda_{\text{i}}/c)(1/h)\right)v_{\text{i}} + (\lambda_{\text{i}} + \lambda_{\text{m}}) + (2\lambda_{\text{i}}/c)(1/h) + 2} \tag{6}$$

with c representing the radius of inclusions and $1/h$ the contact resistance. When h tends towards infinity, the interfacial resistance becomes negligible and we obtain the original Maxwell–Eucken equation.

For higher volume fractions of inclusions, it may be necessary to take into account contact between the inclusion particles yielding a certain connectivity of the second phase. For such cases, Landauer's effective medium expression[10] is of interest and is given by

$$\lambda_{\text{eff}} = \frac{1}{4}\left[\lambda_{\text{i}}(3v_{\text{i}} - 1) + \lambda_{\text{m}}(3v_{\text{m}} - 1) + \sqrt{\left[\lambda_{\text{i}}(3v_{\text{i}} - 1) + \lambda_{\text{m}}(3v_{\text{m}} - 1)\right]^2 + 8\lambda_{\text{m}}\lambda_{\text{i}}}\right] \tag{7}$$

For values of $v_{\text{i}} < 0.15$, Eq. (7) yields almost identical results to the Maxwell–Eucken expression and then for $v_{\text{i}} > 0.15$, there is a stronger influence of the inclusions on the thermal conductivity as they become connected. In fact, Landauer's expression has been used to describe rather successfully the thermal conductivity of zirconia ceramics containing up to 60% of essentially open porosity[11].

4. Results and discussion

4.1. Thermal conductivity of the glass matrix

For the isotropic glass matrix, λ was measured by both the mirage and the laser flash technique. The thermal conductivity value measured by the laser flash technique for the glass matrix ($1.4\ \text{W m}^{-1}\ \text{K}^{-1}$) revealed less than 5% dispersion over a series of 15 measurements (Table 1) and was chosen for the theoretical calculations (λ_{m}). This is also because the effective thermal conductivity of the two-phase samples was characterised with the same technique.

4.2. Thermal conductivity of alumina beads

The small diameter of the alumina inclusions and their shape means that the laser flash technique is not suitable. We have

Table 1
Porosity, average grain size and thermal conductivity of the glass matrix, alumina inclusions and alumina AL23

	Glass matrix	Alumina inclusions	Alumina AL23
Bulk density (kg m^{-3})	2540 ± 5	3980 ± 5	3980 ± 5
Porosity (vol.%)	<0.1	<0.5	<0.5
Linear average grain size ϕ_{grain} (μm)	–	3	5–6
C_p (J kg^{-1} K^{-1})	746	771	771
λ [laser flash technique] (W m^{-1} K^{-1})	1.40 ± 0.06	–	34 ± 1
λ [mirage set-up] (W m^{-1} K^{-1})	1.00 ± 0.25	26 ± 5	29 ± 5
λ [prediction, Eq. (4)] (W m^{-1} K^{-1})	–	29	33

therefore use two complementary approaches to evaluate the thermal conductivity of the alumina beads.

First, a dense alumina disc sample (AL23, Degussit) suitable for the laser flash experiment was analysed. This material exhibits similar chemical and microstructural characteristics to the alumina beads. The density is approximately 3980 kg m^{-3} (Table 1) and the average grain size determined from scanning electron microscopy pictures (Fig. 2a) is in the range of 5–6 μm. The alumina beads exhibit a similar density, corresponding to less than 0.5% porosity, and a slightly smaller average grain size of 3 μm (Fig. 2b).

The thermal conductivity of the AL23 sample was then evaluated with the laser flash technique to be 34 W m^{-1} K^{-1} (Table 1). This value can be compared to 33 W m^{-1} K^{-1} predicted by equation 4 using values for the single crystal thermal conductivity[12] of 35 W m^{-1} K^{-1} and 1.0×10^{-8} m^2 K W^{-1} for the grain boundary thermal resistance. The difference between theory and experiment is within experimental error. Eq. (3) was then used to predict a value of 29 W m^{-1} K^{-1} for the alumina beads, explained by the larger number of interfaces.

Second, the thermal conductivities of the AL23 sample and the alumina beads in the glass matrix were evaluated with the mirage technique (Table 1). This approach yielded slightly lower values of thermal conductivity compared to the predictions but with a similar difference of 10–12% between the AL23 sample and the alumina beads. The important advantage is that the thermal response of the beads has been characterised "in situ" with respect to the surrounding glass matrix. In order to be consistent, the predicted value of 29 W m^{-1} K^{-1} is then chosen to represent the thermal conductivity of the alumina beads (λ_i) for the subsequent calculations because the effective thermal conductivities of glass-alumina mixtures have been evaluated with the laser flash technique.

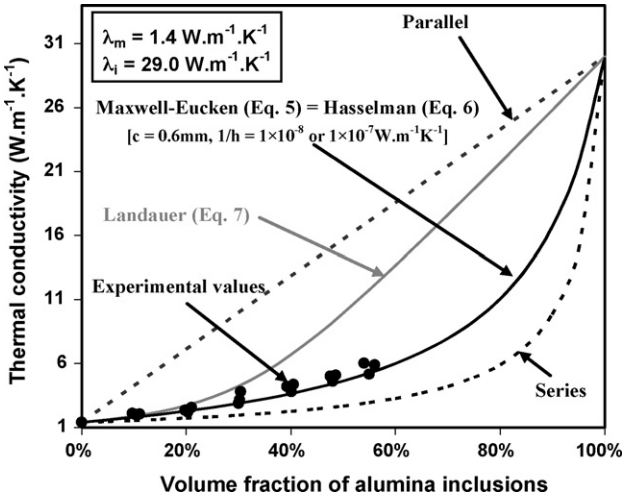

Fig. 3. Effective thermal conductivity vs. volume fraction of alumina inclusions: comparison between experimental values and predictive models.

4.3. Effective thermal conductivity of two-phase materials

Experimental and predicted values of the effective thermal conductivity of alumina inclusion/glass matrix materials are presented in Table 2. Fig. 3 shows that for volume fractions less

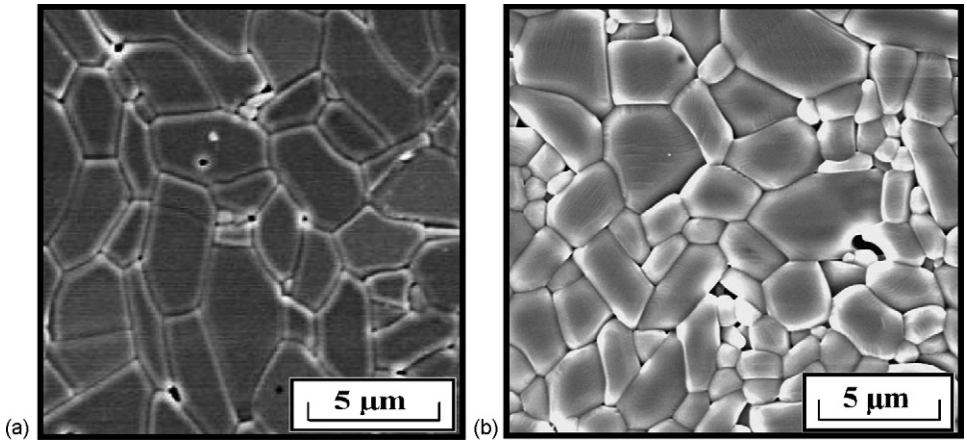

Fig. 2. Microstructures of (a) AL23; (b) alumina inclusions.

Table 2
Density, volume fraction of inclusions and effective thermal conductivity of alumina inclusion/glass matrix samples

Sample	Volume fraction of inclusions in the initial bar (%)	Final measured bulk density (kg m^{-3})	Real volume fraction of inclusions in disc samples (%)	Thermal conductivity (laser flash technique) (W m^{-1} K^{-1})
B-1	10	2680	9.7	2.1
B-2		2687	10.2	2.0
B-3		2700	11.1	2.0
C-1	20	2832	20.3	2.2
C-2		2825	19.8	2.4
C-3		2842	21.0	2.6
D-1	30	2972	30.0	2.9
D-2		2975	30.2	3.2
D-3		2978	30.4	3.8
E-1	40	3104	39.2	4.2
E-2		3117	40.1	3.8
E-3		3123	40.5	4.4
F-1	48	3224	47.5	5.0
F-2		3231	48.0	4.6
F-3		3240	48.6	5.1
G-1	55	3335	55.2	5.2
G-2		3318	54.0	6.0
G-3		3340	56.1	5.9

than 30%, experimental values of thermal conductivity are in good agreement with both the Maxwell–Eucken expression and Landauer's expression. Between 30% and 55% volume fractions, Landauer's expression predicts values, which are significantly higher than the experimental data, which follow closely Eq. (5). This result suggests that the inclusions do not interact enough to allow the establishment of a thermally connected path (percolation) for the alumina phase, even if the average distance separating two consecutive inclusions reduces as the volume fraction increases. Examination of the microstructure of a high alumina content sample (Fig. 4) shows that each bead is surrounded by the matrix phase. In essence, a minimum thickness of this matrix phase limits significantly the possibility of physical contact. In fact, the process of fabrication ensures complete coating of beads during mixing because a good adherence of powder to the beads is obtained with the organic additives.

Fig. 3 also shows that, with a value of thermal resistance for the glass/alumina interface between 1×10^{-8} and 1×10^{-7} m^2 K W^{-1} (the lowest bound corresponding to average grain boundary thermal resistance measured for alumina) and a mean diameter of 0.6 mm for alumina beads, predictions with Hasselman's expression merge with the Maxwell–Eucken curve. This implies that the thermal resistance at the inclusion/matrix interface does not affect significantly the effective thermal conductivity of two-phase samples. A significant variation of the effective thermal conductivity would have been obtained if the ratio $\lambda_i/(ch)$ has a value of 10 or greater. In other words, in the present case the interfaces exhibit a good contact and are small in number due to the millimetre size of the beads ($c \approx 0.6$ mm). The conclusion would be modified if the inclusions were smaller, increasing the contribution of the contact resistance term in Hasselman's expression. It would be also modified in the case of a thermal expansion mismatch between the inclusions and the matrix.

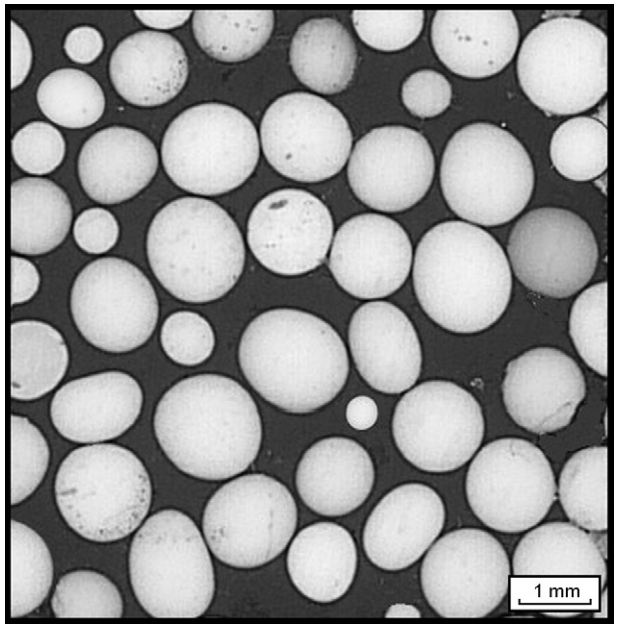

Fig. 4. Microstructure of a glass/alumina sample (alumina volume fraction ≈ 55%).

5. Conclusions

The effective thermal conductivity of a two-phase system constituted of isolated spherical alumina particles in a glass matrix has been measured with the laser flash technique. Prior

to that, the thermal conductivity of the mm sized alumina inclusions was evaluated at a local scale with the mirage technique, revealing no significant modification due to the presence of the surrounding glass matrix. However it was necessary to take into account the average grain boundary thermal resistance and the grain size in the value attributed to the polycrystalline alumina phase with small (μm) sized grains. The Maxwell–Eucken expression was then shown to describe successfully the effective thermal conductivity of the glass/alumina mixtures for alumina volume fractions up to 55%. In essence for all samples the microstructure can be simplified to a single isolated conducting spherical inclusion, representing alumina, in the insulating glass matrix. Hasselman's correction to the Maxwell–Eucken expression, taking into account the effect of thermal resistance at the glass/alumina interface, is not needed because of the large (mm) size of the inclusions. The divergence, between the experimental values of thermal conductivity and predictions by Landauer's effective medium expression, for alumina volume fractions above 20% confirms the absence of connectivity between the conducting alumina particles.

In the future we wish to investigate the role of thermal expansion mismatch between the two solid phases on the effective thermal conductivity of the system.

Acknowledgements

Nicolas Tessier–Doyen would like to thank the French Ministry of Research and Technology for the PhD study grant.

References

1. Fayette, S., Conduction thermique dans les matériaux hétérogènes: influence des joints de grains, Ph.D. Thesis, University of Limoges, France, 2001.
2. Tessier-Doyen, N., Glandus, J. C., Huger, M., Experimental and numerical study of elastic behaviour of heterogeneous model materials with spherical inclusions. *J. Mater. Sci*., in press.
3. Parker, W. J., Jenkins, R. J., Butler, C. P. and Abbot, G. L., Flash method of determining thermal diffusivity, heat capacity, and thermal conductivity. *J. Appl. Phys.*, 1961, **32**, 1679–1684.
4. Knacke, O., Kubaschewski, O. and Hesselmann, K., *Thermal chemical properties of inorganic substances* (*2nd ed.*). Springer-Verlag, Berlin, 1976.
5. Charbonnier, F. and Fournier, D., A compact design for photothermal deflection (mirage) spectroscopy and imaging. *Rev. Sci. Instrum.*, 1986, **57**, 1126–1132.
6. Smith, D. S., Fayette, S., Grandjean, S. and Martin, C., Thermal resistance of grain boundaries in alumina ceramics and refractories. *J. Am. Cer. Soc.*, 2003, **86**(1), 105–111.
7. Maxwell, J. C., *Treatise on electricity and magnetism* (*1st ed.*). Clarendon Press, Oxford, 1873.
8. Eucken, A., Thermal conductivity of ceramics refractory materials. *Forsch. Geb. Ing., B-3, Forschung Sheft*, 1932, **53**, 6–21.
9. Hasselman, D. P. H. and Johnson, L. F., Effective thermal conductivity of composites with interfacial thermal barrier resistance. *J. Comp. Mat.*, 1987, **21**, 508–515.
10. Landauer, R., The electrical resistance of binary metallic mixtures. *J. Appl. Phys.*, 1952, **23**(7), 779–784.
11. Naït-Ali, B., Haberko, K., Vesteghem, H., Absi, J. and Smith, D. S., Thermal conductivity of highly porous zirconia. *J. Eur. Ceram. Soc.*, 2006, **26**(16), 3567–3574.
12. Goldsmith, A. *et al.*, Handbook of thermophysical properties of solid materials. In ed. A. Goldsmith, T. E. Waterman and H. J. H. Hirschhorn. In *Ceramics*, *III*. MacMillan Company, New York, 1961.